6.4

LABORATORY STUDIES OF STIRRING BY SMALL-SCALE GEOSTROPHIC MOTIONS

Grant A. Stuart
Miles A. Sundermeyer*
University of Massachusetts Dartmouth, New Bedford, Massachusetts

David Hebert
University of Rhode Island, Narragansett, Rhode Island

Abstract: **We report the results of laboratory experiments examining the adjustment of diapycnal mixing events, and their effect on lateral dispersion in the ocean's stratified interior. Vertically oscillated mesh grids were used to produce localized mixed patches that adjusted to form stable, geostrophically balanced eddies within a rotating, linearly stratified fluid. The effective lateral dispersion due to many such events showed a linear dependence on the frequency of mixing events, and higher order dependence on Burger number, consistent with previous theoretical and numerical results. Results also suggest, however, a revised form of the effective lateral diffusivity parameterization to extend previous results to a more general non-geostrophic form.**

1. INTRODUCTION

Stirring by small-scale geostrophic motions, or the vortical mode, is hypothesized to play a significant role in small-scale lateral mixing in the ocean's stratified interior (Polzin et al., 2003; Sundermeyer et al., 2005). Sub-mesoscale eddies are presumed to form due to the geostrophic adjustment of mixed patches following diapycnal mixing events (e.g. breaking internal waves) within a stratified water column (McWilliams, 1988; Sundermeyer et al., 2005; Sundermeyer and Lelong, 2005). Sundermeyer et al. (2005) recently derived order-of-magnitude estimates of the effective lateral dispersion resulting from such motions using simple geostrophic scaling combined with a random walk. They estimated that on scales of 1-10 km in the stratified waters of the continental shelf, lower-bound estimates of the effective lateral diffusivity by this mechanism ranged from 1 to 10 $m^2 s^{-1}$.

In the present study, laboratory experiments were used to model the dynamical sequence of events driving vortical mode stirring described by Sundermeyer et al. (2005). Specifically, results from dye and PIV (Particle Imaging Velocimetry) measurements were analyzed to confirm the dynamics of the geostrophic adjustment problem for the time and space scales of interest, and to test the hypothesized parameter dependence of the effective lateral diffusivity by such motions.

2. EXPERIMENTAL SETUP

Two sets of experiments were conducted. The first was aimed at confirming the dynamics of the adjustment of an individual mixed patch in terms of its size and strength, and the relation of these to the initial mixed patch parameters, namely the height, h, the width, L, the background stratification, N, and rotation, f. The second set of experiments then examined the dependence of the effective lateral dispersion on these same parameters, and the effective frequency of mixing events, ϕ.

Experiments were conducted on a high-precision rotating table at the University of Rhode Island's Graduate School of Oceanography. The table rotated counter-

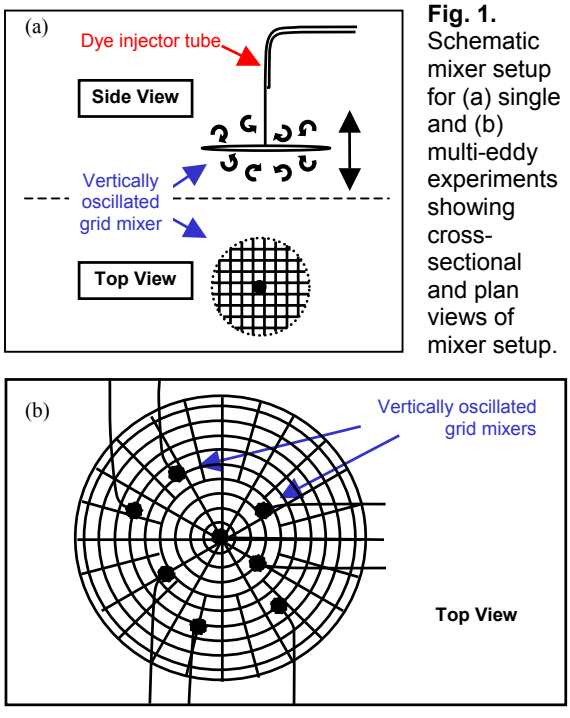

Fig. 1. Schematic mixer setup for (a) single and (b) multi-eddy experiments showing cross-sectional and plan views of mixer setup.

* *Corresponding author address:* Miles A. Sundermeyer, Univ. Massachusetts Dartmouth, Dept. of Estuarine and Ocean Sciences, 706 S. Rodney French Blvd., New Bedford, MA 02744; e-mail: msundermeyer@umassd.edu.

clockwise as viewed from above, and was equipped with electrical and fluid slip rings to allow power and water to be supplied to the table while rotating. A superstructure mounted on the table allowed flow visualization technology (on board PC, digital cameras, laser and power supply, dye injector, etc.) to rotate within the table's reference frame.

The tank was a cylindrical Plexiglas tank (D = 1.0 m, H = 0.48 m). To correct for optical distortions of side views, the cylindrical tank was placed within a larger square tank, and the space between the two filled with fluid of the same density and stratification. An angled mirror situated at the side of the tank enabled both plan and side views to be captured by overhead cameras. A Plexiglas lid was used to eliminate wind stress effects on the fluid surface.

Localized mixed regions of fluid were formed by vertically oscillating a horizontal grid positioned at mid-depth (d = 15 cm, Fig. 1). The stainless steel mesh grid was a 5.08-cm diameter circular disk that was painted with a mixture of black and rhodamine WT fluorescent dye to minimize scattering off the mixer during PIV visualization. A slider-crank mechanism was used to oscillate the mixing grids through a vertical stroke distance of 3.0 cm at a frequency of approximately 1.0 Hz. Each mixer was activated for 25 seconds to ensure that the mixed patch was thoroughly mixed, so that the stratification anomaly, ΔN, was of order the background stratification itself.

Green food coloring (mixed with ethyl alcohol to achieve neutral buoyancy) was used as a passive tracer to track the adjustment evolution and to estimate eddy velocities in the single eddy experiments. A syringe pump injected the dye at 60 ml/hr for 3 table rotations at the equilibrium depth. A Canon Powershot G6 7.1 megapixel digital still camera was used to take high-resolution images of the dye during the experiments. The evolution of the dye patch was also recorded continuously using a Panasonic MiniDV digital video camcorder.

Particle Image Velocimetry (PIV) was used as a second means of studying the flow evolution of the single eddy adjustment and to obtain precise measurements of the velocity field. The PIV system consisted of a twin cavity Nd:YAG laser (Neodymium-doped Yttrium Aluminium Garnet crystal) and two LaVision® FlowMaster® CCD cameras bandpass filtered to detect only the laser wavelength. A 2.0 mm-thin horizontal laser light sheet illuminated the target depth at d = 15 cm. Neutrally buoyant tracer particles (silver coated glass spheres) were added to the fill tanks prior to each fill. PIV images were taken 10 times per table rotation for 20-30 inertial periods.

Table 1. List of parameter values for the base run.

Variable Name	Symbol	Oceanic value	Scaled lab value
Coriolis parameter	f	10^{-4} rad/s	0.25 rad/s
Buoyancy frequency	ΔN	18 cph	490 cph
patch half-height	h	5.0 m	5.0×10^{-2} m
patch radius	L	370 m	4.0×10^{-2} m
Deformation radius	R_D	1600 m	0.17 m
Burger #	Bu	18	18
Ekman #	Ek	5.6×10^{-4}	1.5×10^{-2}

3. SINGLE EDDY EXPERIMENTS

3.1. Base Run

Parameter values for an experimental base run are listed in Table 1 with corresponding realistic oceanic values based on observations made during the Coastal Mixing and Optics dye-release experiments (Sundermeyer et. al, 2005). Scaled lab values were based on considerations of realistic oceanic values, laboratory imposed constraints, and to preserve the relevant nondimensional numbers, in this case the Burger number and the Ekman number. Although the laboratory experiments ended up having larger Ekman number than real ocean values, it was still much less than 1, so that laboratory eddies still adjusted rotationally, as opposed to frictionally.

The adjustment of an isolated mixed patch as revealed by dye for the base case parameters is shown in Fig. 2. The time evolution shows the radial growth of the dye patch over 3 inertial periods. From dye wisps visible at 35 s into the experiment, anticyclonic rotation is clearly discernible. (Note that the other grid mixers visible in the field of view were never actuated during this run.) From these dye images, representative length and velocity scales were estimated for the adjustment. The representative length scale was estimated by subtracting the initial length scale of the mixed patch from the adjusted eddy radius to calculate a displacement, $d = L_f - L_i$. For the base case, this yielded $d = 0.088 \pm 0.016$ m, which was about a factor of 2 smaller than the value predicted by the analytical solution of McWilliams (1988) for the cyclo-geostrophic adjustment of an initial parabolic lens with no velocity and 5 active layers. Meanwhile, a characteristic eddy velocity estimated by tracking distinct features in the dye gave a value

of V_{max} = 0.0024 ± 0.0006 m/s, i.e., about a factor of 3 smaller than the value predicted by McWilliams's (1988) solution.

PIV images of the mixed patch adjustment for the same base case parameters are shown in Fig. 3 (note the different time intervals of the images compared to Fig. 2). The initial turbulent action of the grid mixer is clearly visible in the first two images, followed shortly by the formation of a stable anti-cyclonic eddy, and eventually by its frictional decay. From these PIV vector fields, a second estimate of a representative length scale of the adjustment was taken as the radius of maximum velocity, which for this run was r_V = 0.052 ± 0.005 m. This was approximately a factor of 2 smaller than the length scale estimated from the dye. A second estimate of a representative eddy velocity was also obtained from the PIV velocity fields. This was done by azimuthally averaging the observed velocity magnitude, $V_{max} = \mathrm{sqrt}(u^2 + v^2)$, in a band Δr = ± 0.5 cm about the estimated radius of maximum velocity. The characteristic velocity scale for the base case (estimated within the first 2 inertial periods after the mixing stopped) was V_{max} = 0.0026 ± 0.0007 m/s, consistent with the velocity estimated from the dye.

3.2. Additional Runs

To explore the parameter dependence of geostrophic adjustment for subsurface mixed patches, a suite of experiments was conducted

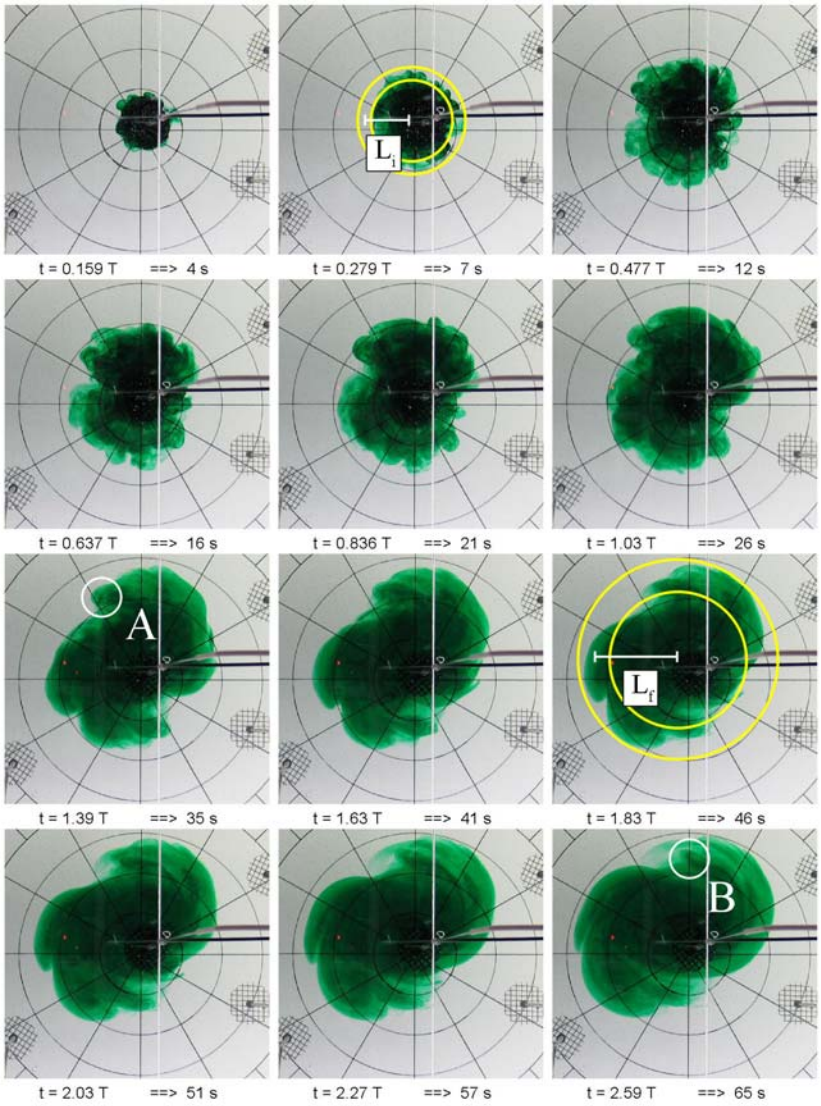

Fig. 2. Plan view time evolution photographs of a single eddy adjustment (f = 0.25 rad/s, ΔN = 0.86 rad/s). Concentric yellow circles indicate estimates of the maximum and minimum extent of the mixed patch (t = 7s) and the adjusted eddy radius (t = 46 s). The start (A) and end (B) positions used to estimate the angular displacement of one noticeable eddy feature are identified with white circles. Note the irregular time spacing between successive snap-shots.

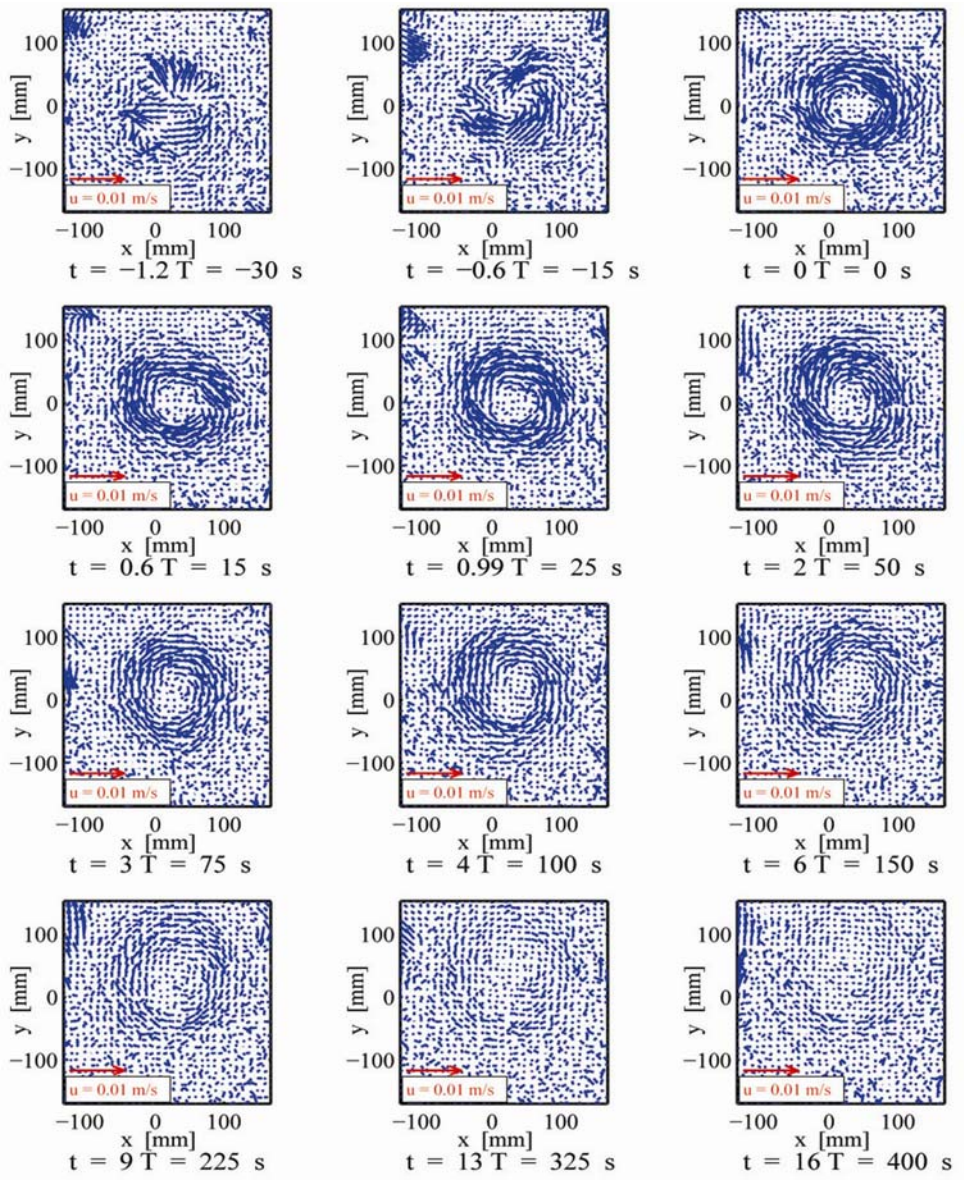

Fig. 3. Plan view time evolution PIV fields from a single eddy adjustment (f = 0.25 rad/s, ΔN = 0.86 rad/s). The 5-cm region of near zero velocity at the center of the eddy corresponds to false image correlations of the motionless mixer, i.e., not necessarily the true eddy core velocity. Note the irregular time spacing between successive snapshots.

in which the initial parameters of the mixed patch were systematically varied. Specifically, experiments were run doubling and halving f holding ΔN constant, doubling ΔN holding f constant, and doubling both ΔN and f. Again, characteristic lengths and velocities from these experiments were compared to analytical solutions by McWilliams (1988).

Observed adjustment length scales from the single eddy experiments plotted against their corresponding R_D/L ratios are shown in Fig. 4 The Rossby radius, $R_D=\Delta N\, h/f$, is indicated as a constant value (i.e., a horizontal line at 1.0) on the displacement axis. McWilliams's (1988) solution is also shown, approaching R_D (i.e., simple geostrophic scaling) for $Bu \sim 1$ and tailing off to smaller values for $Bu << 1$ and $Bu >> 1$. Comparing the results for different Bu, the laboratory results show overall agreement (to within a constant scale factor; see above) with the analytical solutions for $Bu >> 1$, namely a decrease in the adjustment length scale with increasing Bu.

The observed adjusted velocities plotted against corresponding R_D/L ratios for each experiment are shown in Fig. 5. Geostrophic velocity scaling, $U_g=\Delta N h/fL$, based on initial parameters is indicated as a constant value (i.e., a horizontal line at 1.0) on the velocity axis. Here, McWilliams's (1988) solution asymptotes to V_g for $Bu << 1$, tailing off with a negative slope for $Bu >> 1$. Comparing the results for different Bu to the analytical solutions, again the

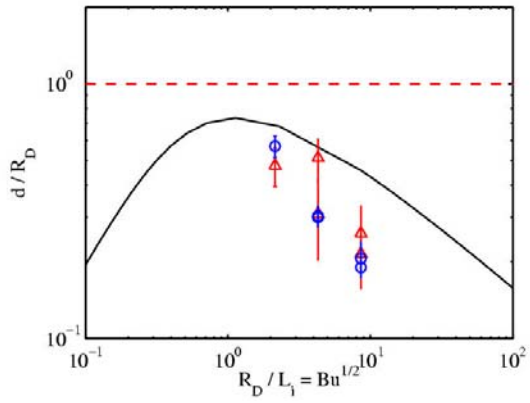

Fig. 4. Length scale (d) vs. Burger number (Bu). Observed adjustment length scales are plotted against corresponding R_D/L ratios. Data from both dye (Δ) and PIV (**o**) experiments are plotted, normalized by R_D. Simple geostrophic displacement scaling, R_D, (- -) and McWilliams's (1988) solution (—) are also shown.

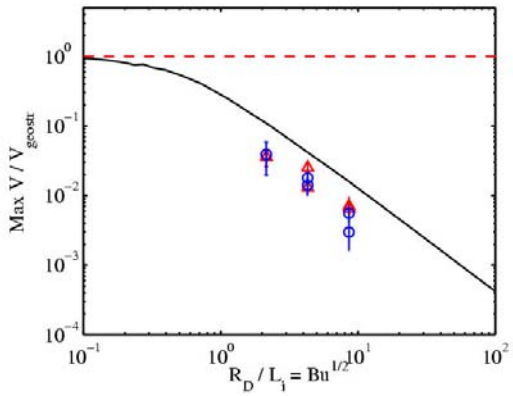

Fig. 5. Velocity scale ($\mathbf{V_{max}}$) vs. Burger number (Bu). Observed velocities plotted against corresponding R_D/L ratios. Data from both dye (Δ) and PIV (**o**) experiments are plotted. Geostrophic velocity scaling (- -) and McWilliams's (1988) solution (—) are also shown.

laboratory results show approximate agreement (to within a constant scale factor) with the analytical solutions for *Bu* >> 1, namely a decrease in the adjusted velocity with increasing *Bu*.

4. MULTI-EDDY EXPERIMENTS

4.1. Base Run

From the single eddy experiments, as well as the theoretical solutions of McWilliams (1988), it is clear that the adjustment velocity of an eddy is dependent on the Burger number (*Bu*) and that simple geostrophic velocity scaling (i.e., $U_g = \Delta Nh/fL$) is not valid for the entire dynamical range of adjustments. We therefore next examined how the Burger number dependence of velocity effects the effective lateral diffusivity parameterization of Sundermeyer et al. (2005) for a field of multiple such eddies.

The parameters for the multi-eddy base run were identical to the single eddy base run except for the additional ϕ parameter, which indicates the frequency of mixing events at a given location in the water column. In the present experiments, the latter was approximated as the time between individual mixing events, $1/\Delta T_{MIX}$.

The evolution of the dye for the base case multi-eddy run is shown in Fig. 6. The sequence of snap-shots shows the evolution of the tracer, from the initial mixed patch to its gradual straining and streaking, until it ultimately fills the tank. Beyond the qualitative information obtained from the series of digital photographs, digital image processing was used to quantify the growth of the dye variance for each run based on the area stained and the intensity relative to background. From this, second moments of the tracer along and across the major axis of the patch were used to estimate the time rate of change of the variance, and hence the effective lateral diffusivity of the dye. For the base case, the estimated effective diffusivity estimated from the dye was $\kappa_H = 2.3 \pm 0.3 \times 10^{-5}$ m^2/s. This was one order of magnitude smaller than predicted by the Sundermeyer et al. (2005) κ_H scaling, and an order of magnitude larger than predicted by a modified scaling using the McWilliams (1988) analytical solution for velocity in the same scaling.

4.2. Additional Runs

Two sets of experiments were used to test the parameter dependence of the effective lateral diffusivity compared to theoretical predictions. The first set of experiments varied the event frequency, ϕ, to test the linear parameter dependence. The second set examined various combinations of ΔN and *f* to test the parameter dependence on Burger number. In all of these, the base case run parameters were the same as those used in the single eddy base run.

The observed κ_H as measured from the dye as a function of the inverse interval between mixing events, $1/\Delta T_{MIX}$, is shown in Fig. 7. Consistent with theoretical expectations, the results show a clear linear dependence across an order of magnitude variation in $1/\Delta T_{MIX}$.

The observed diffusivity values for the κ_H vs. *Bu* experiments are shown in Fig. 8. Here, all values of diffusivity were normalized by the scaling of Sundermeyer et al (2005) using the initial parameters of each run. Here the

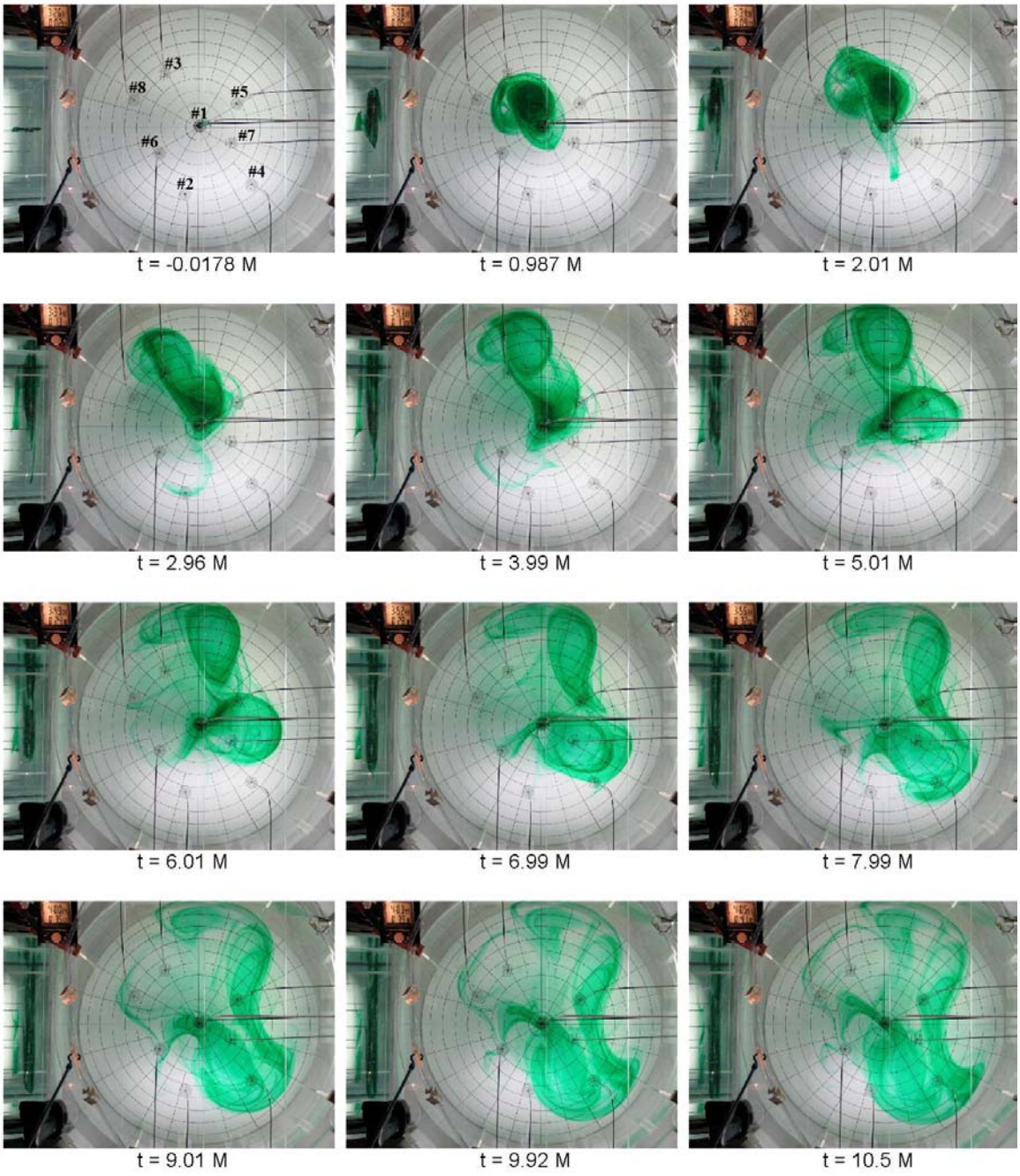

Fig. 6. Plan view time evolution photographs of the base experimental run for the multi-eddy stirring experiment (f = 0.25 rad/s, ΔN = 0.8587 rad/s, ϕ = 0.0044 s^{-1}). Frame one (t = - 0.0176 M) indicates the activation sequence for each mixer. M corresponds to the time interval between mixing events. (In this instance, M = 225 s)

Sundermeyer et al (2005) scaling is indicated as a constant value (i.e., 1.0) on the diffusivity axis. A modified Sundermeyer et al (2005) diffusivity scaling using the McWilliams (1988) solution for velocity is also indicated. The latter asymptotes to the Sundermeyer et al. (2005) scaling for *Bu* << 1 and tails off with a negative slope for *Bu* >> 1. Most notable in the figure is that the laboratory results show a distinct 'tail-off' in diffusivity similar to the McWilliams (1988) modified diffusivity solution, although the slope of the laboratory results is somewhat steeper than the latter.

5. SUMMARY AND CONCLUSIONS

The adjustment of an isolated mixed patch in a continuously stratified environment was shown to be consistent both qualitatively and quantitatively with analytical solutions for an axisymmetric lens. Specifically, results for the single eddy experiments showed adjusted length

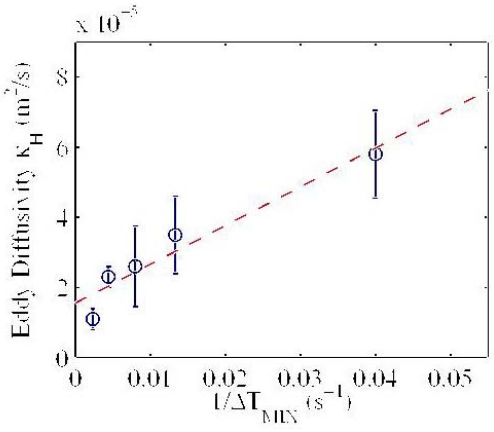

Fig. 7. Observed κ_H vs. mixer frequency, $\phi = 1/\Delta T_{MIX}$.

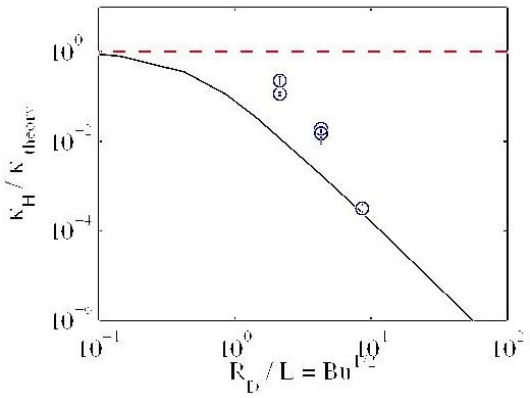

Fig. 8. Observed κ_H vs. Burger number, *Bu*. Red dashed line indicates the Sundermeyer et al. (2005) scaling, black dash-dot indicates modified scaling using McWilliams's (1988) velocity solution. All κ_H values have been normalized by Sundermeyer et al. (2005) scaling.

and velocity scales, consistent with the analytical solution of similar geometry by McWilliams (1988) for Burger number > 1 and R_D/L ratios spanning approximately and order of magnitude.

Multi-eddy stirring experiments incorporating the same dynamics demonstrated for the first time in the laboratory how episodic diapycnal mixing in a linearly stratified water column produces geostrophic eddies that combined to drive horizontal dispersion of a passive tracer. Diffusivities inferred from these experiments indicated a positive linear relationship with changing event frequency, ϕ, consistent with the dependence predicted by scaling. The observed diffusivities from a series of κ_H vs. *Bu* experiments further indicated a parameter dependence consistent with a modified form of the Sundermeyer et al. (2005) theoretical diffusivity in which the McWilliams (1988) solution for velocity was used in place of simple geostrophic velocity scaling. This modified scaling was shown to be more representative of the laboratory diffusivity data for *Bu* > 1.

ACKNOWLEDGEMENTS

The authors thank Jim Fontaine and Joe Kuehl for their assistance in the laboratory, and Chris Luebke for early work on the mixer design and fabrication. Support for this work was provided by the National Science Foundation Physical Oceanography program under grants OCE-0351892 and OCE-0351905.

REFERENCES

J. C. McWilliams, 1988: Vortex generation through balanced adjustment, *J. Phys. Oceanogr.*, **18**, 1178-1192.

K. L. Polzin, E. Kunze, J. M. Toole, and R. W. Schmidt, 2003: The partition of finescale energy into internal waves and subinertial motions, *J. Phys. Oceanogr.*, **33**, 234-248.

M. A. Sundermeyer, J. R. Ledwell, N. S. Oakey, and B. J. W. Greenan, 2005: Stirring by small-scale vortices caused by patchy mixing, *J. Phys. Oceanogr.*, **35**, 1245-1263.

Sundermeyer, M. A., and M. P. Lelong, 2005: Numerical simulations of lateral dispersion by the relaxation of diapycnal mixing events. *J. Phys. Oceanogr.*, **35**, 2368-2386.